Substantial Intramolecular Charge Transfer Induces Long Emission Wavelengths and Mega Stokes Shifts in 6-Aminocoumarins

Xiaogang Liu,[*,†,‡,§] *Jacqueline M. Cole,*[*,†,⊥,∥,▽] *Zhaochao Xu*[*,#]

[†]Cavendish Laboratory, Department of Physics, University of Cambridge, J. J. Thomson Avenue, Cambridge, CB3 0HE, UK

[‡]Singapore University of Technology and Design, 8 Somapah Road, Singapore 487372, Singapore

[§] Singapore-MIT Alliance for Research and Technology (SMART), 1 CREATE Way, Singapore 138602, Singapore

[⊥]Department of Chemical Engineering and Biotechnology, University of Cambridge, Philippa Fawcett Drive, Cambridge, CB3 0AS, U.K.

[∥] ISIS Neutron and Muon Facility, STFC Rutherford Appleton Laboratory, Harwell Science and Innovation Campus, Didcot, OX11 0QX, UK.

[▽]Argonne National Laboratory, 9700 S Cass Avenue, Argonne, IL 60439, USA

[#]Key Laboratory of Separation Science for Analytical Chemistry, Dalian Institute of Chemical Physics, Chinese Academy of Sciences, 457 Zhongshan Road, Dalian 116023, China

Abstract

Coumarins are deployed in numerous bioimaging and biosensing applications. Among various coumarin derivatives, 6-aminocoumarins attract increasing attention for their red-shifted emissions, mega Stokes shifts and significant solvatochromism. These spectral characteristics together with weak emission intensities have historically been ascribed to the formation of the twisted intramolecular charge transfer (TICT) state in 6-aminocoumarins. In this work, we demonstrate that it is actually substantial intramolecular charge transfer (ICT) that is responsible for these fluorescent properties. Based on this new understanding, we re-analyzed the sensing mechanism of a 6-aminocouarmin based fluorescent probe and obtained close agreement with experimental data. Our results lead to a deeper understanding on the photophysics of 6-aminocoumarins and will inspire the rational development of novel fluorescent probes.

1 Introduction

Understanding the photophysics of fluorophores is essential to facilitate their widespread applications and enable the rational design of high-performance fluorescent probes. Among various chemical families of fluorophores, coumarin and its derivatives represent one of the most important classes of fluorophores in the blue and green region (Figure 1a).[1] They are deployed in a broad range of bioimaging and biosensing applications,[2-3] while their excellent optical properties also enable numerous uses in dye lasers,[4] non-linear optical materials,[5] and dye-sensitized solar cells.[6-11] The optical spectra of coumarins are often tuned by attaching substituents with varying electron-withdrawing power at position 3 or 4, as well as an electron-donating group at position 7 (Figure 1a).[12-13] A judicious choice of these substituents permits effective control of the "push-pull" effect and intramolecular charge transfer (ICT) characteristics in coumarins, thereby shifting their absorption and emission spectra.[13-17] This well understood mechanism has been applied in the design of many fluorescent sensors. In recent years, increasing attention has also been directed to 6-aminocoumarins, owing to their red-shifted emission wavelengths, considerably large Stoke shifts, and significant solvatochromism. These spectral properties endow 6-aminocoumarins with great potential in multi-color imaging and environmental sensing. Yet, the underlying photophysics of 6-aminocoumarins remains largely controversial.

In a pioneering study, Rettig and Klock proposed that the fluorescent characteristics of 6-aminocoumarins are due to the formation of the twisted intramolecular charge transfer (TICT) state upon photoexcitation.[18] In the proposed TICT state, the amino substituent, which has a roughly planar alignment with respect to the coumarin moiety plane in the ground state (S_0), rotates along the N—C6 axis by ~90°, resulting in a perpendicular alignment in the excited singlet state (S_1). The TICT explanation has subsequently been accepted and referenced by many research

groups.[19-23] In recent years, 6-aminocoumarins have turned out to be a useful platform for developing various fluorescent sensors.[19, 24-28] Along with this rapid development, several research groups started to argue that no direct experimental evidence supports the TICT model in 6-aminocoumarins, using both fluorescence lifetime and pressure-dependent fluorescence intensity measurements as their justification.[24, 29] To discern the working mechanisms of 6-aminocoumarins and facilitate their rational design for high-performance probes, it is thus essential to resolve the controversy over their emission mechanism.

In this paper, we will re-analyze Rettig and Klock's study by employing new (time-dependent) density functional theory (DFT/TD-DFT) calculations on a series of 6-aminocoumarins (Figure 1a). These reveal the limitations of the original quantum chemical calculations performed by Rettig and Klock, and provide an alternative view on the molecular origins of 6-aminocoumarins. We will demonstrate that substantial ICT from the electron-donating group at position 6 on the coumarin scaffold is actually responsible for the unique spectral properties of 6-aminocoumarins, and notably, no TICT occurs during this process. Based on this new understanding, we will re-examine the sensing mechanism of a 6-aminocoumarin derived sensor.

2 Computational Methods

DFT calculations were performed using Gaussian 09.[30] Becke's three-parameter and Lee-Yang-Parr hybrid functional (B3LYP)[31-33] and a 6-31+G(d, p) basis set[34] were used for all calculations, unless stated otherwise. The geometry optimizations of coumarins **1, 4—6** and **8** in both their ground and the first excited singlet states (S_0 and S_1) were performed *in vacuo*. Frequency checks were performed after each geometry optimization to ensure that minima on the potential energy surfaces (PES) were found. Following this, TD-DFT calculations were carried out on the optimized

molecular structures to determine their peak absorption/emission wavelengths and molar extinction coefficients (oscillator strength).

Atomic contributions to the highest occupied molecular orbital (HOMO) and the lowest unoccupied molecular orbital (LUMO) in selected compounds were calculated using Mulliken population analysis, based on the optimized molecular structures in the S_0 state.

The theoretical S_0 and S_1 PES of **4** and **5** *in vacuo* were constructed following the TICT model.[35-37] In these calculations, the dihedral angles (θ, as defined by the average dihedral angle of ∠C5-C6-N-C11 and ∠C7-C6-N-C12 in the case of **4** and that of ∠C6-C7-N-C11 and ∠C8-C7-N-C12 in the case of **5**; see Figure 1a) were fixed at various values, while other geometry parameters were freely optimized employing CAM-B3LYP/6-31+G(d,p) in the S_1 state.[38] The CAM-B3LYP functional describes the overall PES profile accurately in systems involving varied amounts of charge transfer (*i.e.*, when both the ICT and TICT states are of concern).[39] CAM-B3LYP was thus used to construct the PES of **4** and **5**.

3 Results and discussion

3.1 Re-examining the TICT model in 6-aminocoumarins

Rettig and Klock have compared the optoelectronic properties of 6-aminocoumarins and 7-aminocoumarins from experiments, using **2** and **3** as examples (Figure 1a).[18] Even though the emission of **2** is very weak with respect to that of **3**, the Stokes shift of **2** is much larger ($\Delta\lambda$: ~200 nm; $\Delta\nu$: ~9500 cm^{-1}) relative to that of **3** ($\Delta\lambda$: ~80 nm, $\Delta\nu$: ~5200 cm^{-1}); the emission wavelength of **2** (~580 nm) is significantly red-shifted with respect to that of **3** (~430 nm) in alcoholic solvents. In addition, the fluorescence lifetime of **2** is quite long (9.4 ns in acetonitrile). These fluorescent characteristics of **2** are typical "signatures" of TICT emissions. To substantiate the TICT

mechanism, Rettig and Klock performed "molecules-in-molecules" calculations, which showed large amounts of accumulated electron density in position 6 of the LUMO in the parent molecule, coumarin (Figure 1b). Attaching a donor group in position 6 consequently renders TICT energetically more favorable, as strong electrostatic interactions are then possible between the ionized donor group (positive) and the reduced coumarin moiety (negative, especially in position 6). Based on these observations, Rettig and Klock concluded that the emission of **2** should arise from TICT upon optical excitation.

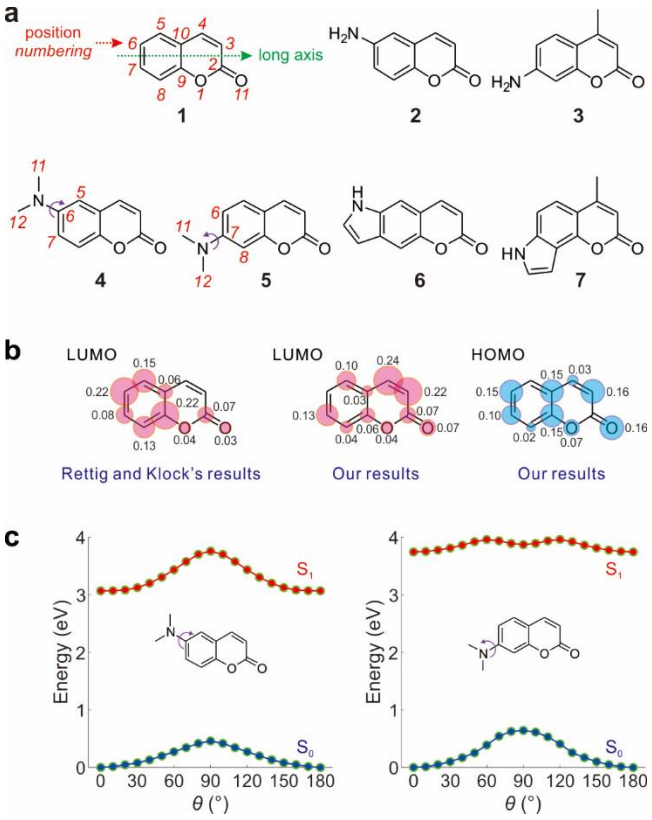

Figure 1. (a) Molecular structures of **1** – **7** and atomic numbering schemes for **1**, **4**, and **5**. (b) Individual atomic contributions to the electron density distributions in the LUMO and HOMO of **1**; the sizes of the blue/red circles are proportional to the atomic contributions, and only contributions greater than 0.02 are shown; Rettig and Klock's results were obtained by normalizing

the squared HMO coefficients reported in reference 18. (c) The S_0 and S_1 PESs of **4** (left) and **5** (right) *in vacuo* as a function of the rotational angle θ.

More than three decades later, the rapid development of high-performance computing and the implementation of more accurate quantum chemical calculation methods (i.e., DFT/TD-DFT) allow us to re-evaluate Rettig and Klock's conclusion. In contrast to their results, our calculations show that the electron density in the LUMO of **1** is actually higher in position 7 than in position 6 (Figure 1b). This suggests that the amino group in position 7 (and not in position 6) is prone to TICT, and previous HMO calculations might be problematic. Indeed, further calculations of the potential energy surface (PES) along the rotational angle of the dimethylamino group in **4** and **5** demonstrated that TICT is energetically unfavorable in position 6, but is potentially accessible in position 7 (Figure 1c). Compounds **4** and **5** are positional isomers that differ only with respect to the position of attachment for the donor substituent (**4**: position 6; **5**: position 7). In the ground states of both **4** and **5**, the torsional angle (θ) between the dimethylamino group and the plane of the coumarin scaffold is approximately 0°. As θ increases to 90°, which corresponds to the TICT state, the S_1 PES of **4** reaches a maximum, concomitant with an energy increase of ~0.69 eV relative to that of the flat ICT state ($\theta = 0$); TICT is thus energetically unfavorable in **4**. In contrast to that, the TICT state of **5** corresponds to a local minimum *in vacuo*. This state often becomes accessible in polar solvents, as strong electrostatic interactions render it more stable than the ICT state.[40]

It should be pointed out here that, so far, emissions from the TICT states of coumarins have not been reported.[37] Moreover, reducing the solvent temperature to 77 K in experiments (which essentially increases the solvent viscosity and potentially reduces molecular rotations) does not

enhance the fluorescence of the 6-substituted aminocoumarin, **2** in ethanol.[18] Conversely, coumarins substituted at position 7, which are susceptible to TICT, exhibit increased fluorescence intensity with increased solvent viscosity.[37] Therefore, it can be concluded that substituents in position 7, but not position 6, facilitate TICT.

One may also consider the photophysical properties of the positional isomers **6** and **7**, which likewise differ only with respect to the position of donor attachment on the coumarin scaffold (Figure 1a). In aqueous solution, their Stokes shifts were measured to be 189 nm (10767 cm^{-1}) and 77 nm (5894 cm^{-1}), respectively; and their emissions peaked at 524 nm and 402 nm, respectively.[19] Yet, the tremendously large Stokes shift and red-shifted emission of **6** cannot be attributed to TICT, as the donating amino substituent is constrained within a fused ring structure. Moreover, **6** possesses a lower quantum efficiency (QE) than **7**.[19] These results indicate that the large Stokes shift, long emission wavelength and low QE of **2** cannot arise exclusively from TICT.

3.2 Revealing the true molecular origins of 6-amino-coumarin photochemistry

To better understand the molecular origins of the different photophysical properties in 6- and 7-substituted coumarins, DFT and TD-DFT calculations were carried out on the ground (S_0), and first excited state (S_1) of **4** and **5**. Firstly, the results showed that the first absorption band in the UV-Vis absorption spectrum of **4** should be located at longer wavelengths compared to that of **5** (Figure 2a). This effect can be rationalized by considering the electron densities in the HOMO and LUMO of **1** (Figure 1b). In position 6 of **1**, the electron density is very high in the HOMO, but decreases distinctly in the LUMO. Therefore, attaching an electron-donating group in position 6 greatly destabilizes the HOMO and reduces the energy of the coumarin bandgap.[41] In contrast, the electron density in position 7 exhibits only minor changes for the HOMO – LUMO transition.

Accordingly, an electron-donating group attached in position 7 induces similarly destabilizing effects in both the HOMO and LUMO, such that the resulting overall change of the energy bandgap should be relatively small.

Secondly, the results showed that the large Stokes shifts in 6-substituted coumarins can be explained well by substantial amounts of ICT upon optical excitation. In **4**, for example, the HOMO – LUMO transition is accompanied by a considerable decrease of electron density around the dimethylamino group in position 6, whereby the corresponding atomic contributions drop from 0.30 to almost 0 (Figure 2b). In contrast, the atomic contributions in **5** decrease less drastically, *i.e.*, from 0.25 to 0.03, indicating smaller extents of ICT (Figure 2b). The amount of ICT in **4** and **5** can furthermore be quantified by the overlap index (Λ) of the HOMO and LUMO electron densities, since the S_1 states predominantly involve HOMO→LUMO transitions, whereby Λ carries a range of 0 to 1 and a smaller Λ corresponds to increased ICT.[42] The obtained DFT results showed a smaller Λ value for **4** (0.5840) compared to that of **5** (0.6635), reflecting a larger extent of ICT in **4** (Table 1). The extent of ICT is positively related to the degree of geometry relaxation in the excited state (since movement of the atomic nucleus follows that of electron flow), and eventually translates into the Stokes shifts of fluorophores. Indeed, the root mean square (RMS) of the cumulative atomic displacements of **4** upon optical excitation is substantially larger than that of **5**, even though these two compounds are positional isomers (Table 1). In view of the large amounts of ICT and associated geometry relaxation upon excitation in 6-substituted coumarins, the observation of a large Stokes shift is hardly surprising (Figure 2a).

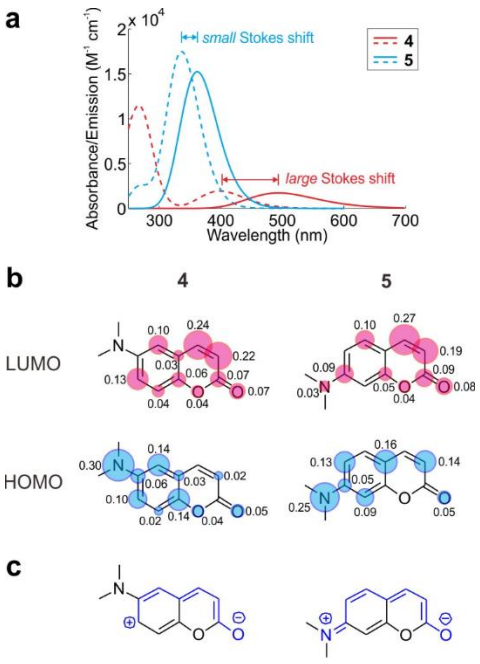

Figure 2. (a) Theoretical UV-Vis absorption (dotted lines) and emission spectra (solid lines) of **4** and **5** *in vacuo*. (b) Individual atomic contributions to the electron density distributions in the LUMO and HOMO of **4** and **5**; the sizes of the blue/red circles are proportional to the atomic contributions, and only contributions greater than 0.02 are shown. (c) Representative resonance structures of **4** (left) and **5** (right).

Table 1. Dipole moments (S_0), electronic excitation energy, oscillator strengths (*f*) during the $S_0 \rightarrow S_1$ transitions, frontier molecular orbital overlap indexes (Λ), root mean square (RMS) of the cumulative atomic displacements upon optical excitations for **4** and **5** *in vacuo*.

Compound	**Dipole moment (S_0) [D]**	**Absorption transition energy**	***f* (absorption)**	**Emission transition energy**	***f* (emission)**	**Λ^a**	**RMS[b] (Å)**
4	7.637	3.1113 eV 398.49 nm	0.0479	2.5118 eV 493.61 nm	0.0425	0.5840	0.142
5	7.460	3.6845 eV 336.51 nm	0.4298	3.4277 eV 361.71 nm	0.3761	0.6635	0.032

[a]Λ is an index used to quantify the frontier molecular orbital overlap during the vertical $S_0 \rightarrow S_1$ excitation of **4** and **5**; Λ is indexed from 0 to 1 and a smaller Λ corresponds to less molecular orbital overlap and more substantial ICT.[42]

[b]RMS measures molecular structure perturbations occurring during excited state geometry relaxation, by comparing the RMS of the cumulative atomic displacements with the molecular structures in the ground state.

Intuitively, the larger ICT in **4** with respect to that in **5** upon optical excitation can be rationalized *via* resonance theory. In **5** (but not in **4**), a full resonance pathway exists for electron delocalization between the amino donor and the ketone acceptor (highlighted in blue; Figure 2c). In other words, the donor group in position 7 participates more effectively in the delocalized π-system of coumarins. This is reflected in a more pronounced partial double-bond character of the N – C7 bond in **5** (1.377 Å), relative to the corresponding N – C6 bond in **4** (1.393 Å). Owing to the more effective electron delocalization, ICT in **5** does not completely drain the electron density around the amino group upon optical excitation, as shown in its LUMO electron density plot. In contrast,

ICT in **4** is more extensive, and the electron density around the donor group in position 6 decreases substantially in the LUMO of **4**.

Finally, more extensive ICT in 6-substituted coumarins affords a smaller oscillator strength (*f*) compared to the 7-substituted analogues (Table 1).[17] The parameter, *f,* is related to the intrinsic fluorescent lifetime (τ_0) *via* the Einstein transition probabilities of spontaneous emissions (eq. 1).[43-44] Owing to its low *f* and low transition energy (*E*) values*,* the τ_0 of **4** is higher than that of **5**. This increased intrinsic emission lifetime allows the competing non-radiative decays to substantially reduce fluorescence, resulting in lower quantum efficiencies in 6-substituted coumarins. Indeed, Krystkowiak *et al.* have shown that hydrogen bond interactions significantly reduce the quantum yield of 6-aminocoumarin.[45-46]

$$\tau_0 = \frac{c^3}{2E^2 f} \qquad \text{eq. 1}$$

where τ_0 is the intrinsic fluorescence lifetime, *c* the speed of light, *E* the transition energy of fluorescence and *f* the oscillator strength. All units are in atomic units.

In summary, the spectral properties and quantum yields of 6-aminocoumarins can be explained well by extensive ICT from the amino group at position 6 to the coumarin scaffold.

3.3 Re-analyzing the sensing mechanisms of 6-aminocoumarin derived fluorescent sensors

Understanding the true molecular origins of ICT allows us to resolve the ostensible "mysteries" that have surrounded the sensing mechanism of 6-aminocoumarin derived fluorescent sensors. To this end, a fluorogenic probe for monoamine oxidases (**8**) represents probably the best example (Figure 3a).

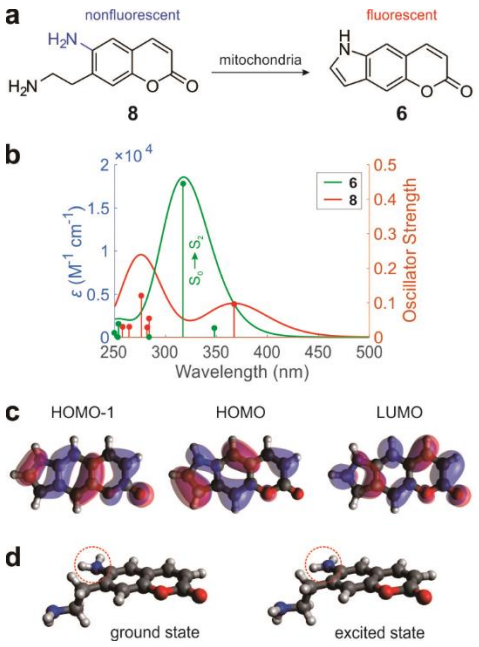

Figure 3. (a) The fluorescence enhancement mechanism of **6** in comparison to **8**. (b) Theoretical UV-Vis absorption spectra and corresponding oscillator strength of **6** and **8** *in vacuo*. (c) Selected molecular orbitals of **6**. (d) Optimized molecular structures of **8** both in the S_0 (left) and the S_1 (right) *in vacuo*; the amino group at position 6 becomes more planar in the excited state (S_1) than in the ground state (S_0), as highlighted in red circles.

Sensor **8** was developed by the Sames group in a seminal work.[19] The design of **8** had been motivated by the limiting TICT rotation of the amino group in position 6 (highlighted in blue) upon forming reactant **6** (Figure 3a). Surprisingly, although the fluorescence brightness of **6** is ~40—50-fold stronger than that of **8**, an ~8-9-fold greater emission manifests in **8** which originates from an enhanced light absorption efficiency; and the quantum efficiency of **6** is only ~5 times as high as that of **8**. In fact, Sames and co-workers have correctly pointed out that the limiting TICT rotation seems to play a minor role (if any) in the fluorescence activation of **8**.

These facts are not surprising at all, in light of our demonstration herein that 6-aminocoumarins (including **8**) do not energetically favor the TICT state (Figure 1c). Furthermore, our DFT/TD-

DFT analysis shows that the first absorption band of **6** is substantially stronger than that in **8**, in good agreement with experimental data (Figure 3b). This strong absorption in **6** is mainly attributed to a significant $S_0 \rightarrow S_2$ transition, which is dominated by a HOMO-1→LUMO transition (Figure 3c). The HOMO-1→LUMO transition in **6** experiences a small amount of ICT, as indicated by their large spatial overlap ($\Lambda = 0.7430$). This large overlap in turn leads to a great molar extinction coefficient in **6**.[17] Finally, the amino group in position 6 of **8** experiences a significant geometry change upon photoexcitation. This group becomes more planar in the excited state than in the ground state, as it loses electron density (Figure 3d). This structural change and associated hydrogen bond interactions are greatly minimized in **6** by rigidifying the amino group. It is thus not surprising to observe a higher quantum yield in **6** than in **8**.

In summary, the fluorescence intensification in **6** with respect to **8** is not due to blocking TICT. Instead, its molecular origins lie in both the ICT tuning (which enhances absorbance) and structural rigidification (which increases the quantum yield) of **6**. In fact, the extent of ICT from the substituent at position 6 to coumarin scaffold plays a vital role in determining the wavelength and intensity of the fluorescence output. Modulating the electron-donating strength of this substituent thus allows the development of a broad range of fluorescent sensors.

4 Conclusions

Our DFT/TD-DFT calculations show that substantial amounts of ICT afford weak emissions and significantly large Stokes shifts and long emission wavelengths in 6-aminocoumarins; these spectral properties are not caused by the formation of the TICT state as previously thought. Our analysis is reinforced by close agreement with experimental data. Moreover, we demonstrate that tuning the strength of ICT allows effective control over the emission intensities in 6-

aminocoumarin derivatives, and permits the development of "off/on" sensors. We believe that these results lead to a deeper understanding on the emission mechanism of 6-aminocouamrins and will inspire the creation of novel fluorescent sensors with enhanced performance.

Author information

Corresponding Author

*Email: xiaogang_liu@sutd.edu.sg; jmc61@cam.ac.uk; zcxu@dicp.ac.cn.

Acknowledgements

XL is indebted to Singapore University of Technology and Design for a Startup Research Grant and Singapore-MIT Alliance for Research and Technology for the SMART Scholar Fellowship. JMC thanks the 1851 Royal Commission for the 2014 Design Fellowship hosted by Argonne National Laboratory where work done was supported by DOE Office of Science, Office of Basic Energy Sciences, under contract No. DE-AC02-06CH11357. ZX is supported by the National Natural Science Foundation of China (21422606).

References

1. Lavis, L. D.; Raines, R. T., Bright Ideas for Chemical Biology. *ACS Chem. Biol.* **2008**, *3*, 142-155.
2. Xu, Z.; Liu, X.; Pan, J.; Spring, D. R., Coumarin-Derived Transformable Fluorescent Sensor for Zn^{2+}. *Chem. Commun.* **2012**, *48*, 4764-4766.
3. Grimm, J. B.; English, B. P.; Chen, J.; Slaughter, J. P.; Zhang, Z.; Revyakin, A.; Patel, R.; Macklin, J. J.; Normanno, D.; Singer, R. H.; Lionnet, T.; Lavis, L. D., A General Method to Improve Fluorophores for Live-Cell and Single-Molecule Microscopy. *Nat. Methods* **2015**, *12*, 244-250.
4. Duarte, F. J.; Hillman, L. W., *Dye Laser Principles, with Applications*; Academic Press Inc.; San Diego, CA, 1990.
5. Moylan, C. R., Molecular Hyperpolarizabilities of Coumarin Dyes. *J. Phys. Chem.* **1994**, *98*, 13513-13516.
6. Hara, K.; Sayama, K.; Arakawa, H.; Ohga, Y.; Shinpo, A.; Suga, S., A Coumarin-Derivative Dye Sensitized Nanocrystalline TiO_2 Solar Cell Having a High Solar-Energy Conversion Efficiency up to 5.6%. *Chem. Commun.* **2001**, 569-570.
7. Hara, K., Dye-Sensitized Nanocrystalline TiO_2 Solar Cells Based on Novel Coumarin Dyes. *Sol. Energ. Mat. Sol. Cells* **2003**, *77*, 89-103.
8. Hara, K.; Wang, Z.-S.; Sato, T.; Furube, A.; Katoh, R.; Sugihara, H.; Dan-Oh, Y.; Kasada, C.; Shinpo, A.; Suga, S., Oligothiophene-Containing Coumarin Dyes for Efficient Dye-Sensitized Solar Cells. *J. Phys. Chem. B* **2005**, *109*, 15476-82.
9. Wang, Z. S.; Cui, Y.; Dan-oh, Y.; Kasada, C.; Shinpo, a.; Hara, K., Thiophene-Functionalized Coumarin Dye for Efficient Dye-Sensitized Solar Cells: Electron Lifetime Improved by Coadsorption of Deoxycholic Acid. *J. Phys. Chem. C* **2007**, *111*, 7224-7230.
10. Wang, Z. S.; Cui, Y.; Hara, K.; Dan-oh, Y.; Kasada, C.; Shinpo, a., A High-Light-Harvesting-Efficiency Coumarin Dye for Stable Dye-Sensitized Solar Cells. *Adv. Mater.* **2007**, *19*, 1138-1141.
11. Wang, Z.-S.; Cui, Y.; Dan-oh, Y.; Kasada, C.; Shinpo, A.; Hara, K., Molecular Design of Coumarin Dyes for Stable and Efficient Organic Dye-Sensitized Solar Cells. *J. Phys. Chem. C* **2008**, *112*, 17011-17017.
12. Reynolds, G.; Drexhage, K., New Coumarin Dyes with Rigidized Structure for Flashlamp-Pumped Dye Lasers. *Opt. Commun.* **1975**, *13*, 222-225.
13. Liu, X.; Cole, J. M.; Waddell, P. G.; Lin, T.-C.; Radia, J.; Zeidler, A., Molecular Origins of Optoelectronic Properties in Coumarin Dyes: Toward Designer Solar Cell and Laser Applications. *J. Phys. Chem. A* **2012**, *116*, 727-737.
14. Horng, M.; Gardecki, J.; Papazyan, A.; Maroncelli, M., Subpicosecond Measurements of Polar Solvation Dynamics: Coumarin 153 Revisited. *J. Phys. Chem.* **1995**, *99*, 17311-17337.
15. Jin, H.; Baker, G. A.; Arzhantsev, S.; Dong, J.; Maroncelli, M., Solvation and Rotational Dynamics of Coumarin 153 in Ionic Liquids: Comparisons to Conventional Solvents. *J. Phys. Chem. B* **2007**, *111*, 7291-7302.
16. Wagner, B. D., The Use of Coumarins as Environmentally-Sensitive Fluorescent Probes of Heterogeneous Inclusion Systems. *Molecules* **2009**, *14*, 210-237.
17. Liu, X.; Xu, Z.; Cole, J. M., Molecular Design of UV–Vis Absorption and Emission Properties in Organic Fluorophores: Toward Larger Bathochromic Shifts, Enhanced Molar Extinction Coefficients, and Greater Stokes Shifts. *J. Phys. Chem. C* **2013**, *117*, 16584-16595.

18. Rettig, W.; Klock, A., Intramolecular Fluorescence Quenching in Aminocoumarines. Identification of an Excited State with Full Charge Separation. *Can. J. Chem.* **1985**, *63*, 1649-1653.
19. Chen, G.; Yee, D. J.; Gubernator, N. G.; Sames, D., Design of Optical Switches as Metabolic Indicators: New Fluorogenic Probes for Monoamine Oxidases (Mao A and B). *J. Am. Chem. Soc.* **2005**, *127*, 4544-4545.
20. Whitaker, J. E.; Haugland, R. P.; Ryan, D.; Hewitt, P. C.; Haugland, R. P.; Prendergast, F. G., Fluorescent Rhodol Derivatives: Versatile, Photostable Labels and Tracers. *Anal. Biochem.* **1992**, *207*, 267-279.
21. Zhu, A.; Wang, B.; White, J. O.; Drickamer, H. G., The Effect of High Pressure on the Twisted Intramolecular Charge Transfer of 2-(4-Dimethylaminonaphthalen-1-Ylmethylene) Malononitrile. *J. Phys. Chem. A* **2003**, *107*, 6932-6935.
22. Sun, Y.; Liu, Y.; Chen, M.; Guo, W., A Novel Fluorescent and Chromogenic Probe for Cyanide Detection in Water Based on the Nucleophilic Addition of Cyanide to Imine Group. *Talanta* **2009**, *80*, 996-1000.
23. Yoshida, S.; Nakamura, Y.; Uchida, K.; Hazama, Y.; Hosoya, T., Aryne Relay Chemistry En Route to Aminoarenes: Synthesis of 3-Aminoaryne Precursors Via Regioselective Silylamination of 3-(Triflyloxy)Arynes. *Org. Lett.* **2016**, *18*, 6212-6215.
24. Dadali, A.; Lang, J.; Drickamer, H., The Effect of Pressure on the Luminescence of the Flexible Dye Molecule 6-Amino-Coumarin in Four Solid Polymeric Media. *J. Photochem. Photobiol. A* **1994**, *84*, 203-205.
25. Guha, S.; Lohar, S.; Bolte, M.; Safin, D. A.; Das, D., Crystal Structure and Interaction of 6-Amino Coumarin with Nitrite Ion for Its Selective Fluorescence Detection. *Spectrosc. Lett.* **2012**, *45*, 225-235.
26. Guha, S.; Lohar, S.; Banerjee, A.; Sahana, A.; Mukhopadhyay, S. K.; Matalobos, J. S.; Das, D., Anthracene Appended Coumarin Derivative as a Cr(III) Selective Turn-on Fluorescent Probe for Living Cell Imaging: A Green Approach Towards Speciation Studies. *Anal. Methods* **2012**, *4*, 3163-3168.
27. Guha, S.; Lohar, S.; Sahana, A.; Banerjee, A.; Safin, D. A.; Babashkina, M. G.; Mitoraj, M. P.; Bolte, M.; Garcia, Y.; Mukhopadhyay, S. K., et al. A Coumarin-Based "Turn-on" Fluorescent Sensor for the Determination of Al^{3+}: Single Crystal X-Ray Structure and Cell Staining Properties. *Dalton Trans.* **2013**, *42*, 10198-10207.
28. Tian, Z.; Cui, S.; Pu, S., A Highly Selective Fluorescent Sensor for Dual Detection of Zn^{2+} and F^- Based on a New Diarylethene. *Tetrahedron Lett.* **2016**, *57*, 2703-2707.
29. Krystkowiak, E.; Dobek, K.; Burdzinski, G.; Maciejewski, A., Radiationless Deactivation of 6-Aminocoumarin from the S_1-ICT State in Nonspecifically Interacting Solvents. *Photochem. Photobiol. Sci.* **2012**, *11*, 1322-1330.
30. Frisch, M. J.; Trucks, G. W.; Schlegel, H. B.; Scuseria, G. E.; Robb, M. A.; Cheeseman, J. R.; Scalmani, G.; Barone, V.; Mennucci, B.; Petersson, G. A., et al. *Gaussian 09*; Gaussian, Inc.; Wallingford, CT, 2009.
31. Stephens, P. J.; Devlin, F. J.; Chabalowski, C. F.; Frisch, M. J., Ab Initio Calculation of Vibrational Absorption and Circular Dichroism Spectra Using Density Functional Fields. *J. Phys. Chem.* **1994**, *98*, 11623-11627.
32. Becke, A. D., Density-Functional Thermochemistry. III. The Role of Exact Exchange. *J. Chem. Phys.* **1993**, *98*, 5648-5652.

33. Lee, C.; Yang, W.; Parr, R. G., Development of the Colle-Salvetti Correlation-Energy Formula into a Functional of the Electron Density. *Phys. Rev. B* **1988**, *37*, 785-789.
34. Rassolov, V. A.; Ratner, M. A.; Pople, J. A.; Redfern, P. C.; Curtiss, L. A., 6-31G* Basis Set for Third-Row Atoms. *J. Comput. Chem.* **2001**, *22*, 976-984.
35. Rettig, W., Charge Separation in Excited States of Decoupled Systems—TICT Compounds and Implications Regarding the Development of New Laser Dyes and the Primary Process of Vision and Photosynthesis. *Angew. Chem. Int. Ed.* **1986**, *25*, 971-988.
36. Grabowski, Z. R.; Rotkiewicz, K.; Rettig, W., Structural Changes Accompanying Intramolecular Electron Transfer: Focus on Twisted Intramolecular Charge-Transfer States and Structures. *Chem. Rev.* **2003**, *103*, 3899-4032.
37. Jones II, G.; Jackson, W. R.; Choi, C. Y.; Bergmark, W. R., Solvent Effects on Emission Yield and Lifetime for Coumarin Laser Dyes. Requirements for a Rotatory Decay Mechanism. *J. Phys. Chem.* **1985**, *89*, 294-300.
38. Yanai, T.; Tew, D. P.; Handy, N. C., A New Hybrid Exchange-Correlation Functional Using the Coulomb-Attenuating Method (CAM-B3LYP). *Chem. Phys. Lett.* **2004**, *393*, 51-57.
39. El-Azhary, A. A.; Suter, H. U., Comparison between Optimized Geometries and Vibrational Frequencies Calculated by the DFT Methods. *J. Phys. Chem.* **1996**, *100*, 15056-15063.
40. Liu, X.; Qiao, Q.; Tian, W.; Liu, W.; Chen, J.; Lang, M. J.; Xu, Z., Aziridinyl Fluorophores Demonstrate Bright Fluorescence and Superior Photostability by Effectively Inhibiting Twisted Intramolecular Charge Transfer. *J. Am. Chem. Soc.* **2016**, *138*, 6960-6963.
41. Higashiguchi, K.; Matsuda, K.; Asano, Y.; Murakami, A.; Nakamura, S.; Irie, M., Photochromism of Dithienylethenes Containing Fluorinated Thiophene Rings. *Eur. J. Org. Chem.* **2005**, *2005*, 91-97.
42. Peach, M. J. G.; Benfield, P.; Helgaker, T.; Tozer, D. J., Excitation Energies in Density Functional Theory: An Evaluation and a Diagnostic Test. *J. Chem. Phys.* **2008**, *128*, 044118.
43. Zhang, X.; Chi, L.; Ji, S.; Wu, Y.; Song, P.; Han, K.; Guo, H.; James, T. D.; Zhao, J., Rational Design of D-Pet Phenylethynylated-Carbazole Monoboronic Acid Fluorescent Sensors for the Selective Detection of A-Hydroxyl Carboxylic Acids and Monosaccharides. *J. Am. Chem. Soc.* **2009**, *131*, 17452-17463.
44. Lukeš, V.; Aquino, A.; Lischka, H., Theoretical Study of Vibrational and Optical Spectra of Methylene-Bridged Oligofluorenes. *J. Phys. Chem. A* **2005**, *109*, 10232-10238.
45. Krystkowiak, E.; Dobek, K.; Maciejewski, A., An Intermolecular Hydrogen-Bonding Effect on Spectral and Photophysical Properties of 6-Aminocoumarin in Protic Solvents. *Photochem. Photobiol. Sci.* **2013**, *12*, 446-455.
46. Krystkowiak, E.; Dobek, K.; Maciejewski, A., Deactivation of 6-Aminocoumarin Intramolecular Charge Transfer Excited State through Hydrogen Bonding. *Int. J. Mol. Sci.* **2014**, *15*, 16628.